Lab on a Chip

RSC Publishing

COMMUNICATION

Spatially resolved electrochemical sensing of chemical gradients†

Cite this: *Lab Chip*, 2013, **13**, 208

Received 18th September 2012,
Accepted 8th November 2012

DOI: 10.1039/c2lc41054k

www.rsc.org/loc

Meghan M. Mensack,[a] John B. Wydallis,[a] N. Scott Lynn Jr.,[b] David S. Dandy[c] and Charles S. Henry*[ac]

Chemical gradients drive a diverse set of biological processes ranging from nerve transduction to ovulation. At present, the most common method for quantifying chemical gradients is microscopy. Here, a new concept for probing spatial and temporal chemical gradients is reported that uses a multi-layer microfluidic device to measure analyte concentration as a function of lateral position in a microfluidic channel using electrochemistry in a format that is readily adaptable to multi-analyte sensing.

Measuring chemical gradients generated by biological systems is critical to understanding complex processes ranging from biological signaling to drug metabolism. Information on the release of biomarkers from living samples can (*i*) help elucidate the mechanisms of how different tissue/cell types interact with one another, (*ii*) demonstrate the effectiveness of pharmaceuticals on *in vitro* systems, and (*iii*) give rapid dose-response information when microfluidic chemical gradient generators are utilized.

Microscopy is the most common method for producing spatially and temporally resolved images of chemical gradients. Unfortunately, microscopy is limited by the need to detect fluorescent or chemiluminescent molecules in biological systems. Other highly sensitive analytical techniques, including MALDI-MS, yield spatially resolved data of biomarkers at low concentrations on tissue and cell cultures;[1] however, the sample cannot survive these analysis processes, making combined spatiotemporal analysis difficult. A system that can spatially and temporally resolve the release of multiple non-fluorescent biomarkers from living tissue and cell cultures in near real-time would be desirable in the study of dose-response relationships, cellular communication mechanisms, and chronic toxicity studies.

[a]*Department of Chemistry, Colorado State University, 1872 Campus Delivery, Fort Collins, Colorado, 80523, USA. E-mail: chuck.henry@colostate.edu; Fax: +1 970-491-1801; Tel: +1 970-491-2852*

[b]*Institute of Photonics and Electronics, Academy of Sciences of the Czech Republic, Prague, Czech Republic*

[c]*Department of Chemical and Biological engineering, Colorado State University, 1370 Campus Delivery, Fort Collins, Colorado, 80523, USA*

† Electronic supplementary information (ESI) available: Design, Fabrication, and Operation of the device. COMSOL Model – convection and diffusion profile. Electrochemical Results. See DOI: 10.1039/c2lc41054k

In recent years the use of microfluidic devices for the delivery of media to cell cultures has become a mainstay in cell biology, primarily due to the ability to provide precise control over both the composition of media as well as the dynamics of media delivery. Flow in microfluidic channels is generally confined to the laminar regime, where due to the small characteristic lengths and limited fluid velocities, Reynolds numbers are often well below one.[2] Laminar flow has been used to deliver concentration gradients of chemoattractants for chemotaxis studies of both mammalian and bacterial cells,[3–5] cytotoxic compounds for pharmacokinetic studies,[6] as well as small molecule gradients with subcellular gradient resolution.[7]

Electrochemical biosensors have many useful properties for measuring chemical gradients in cellular systems because they provide selectivity through either voltage control or surface modification and are capable of measuring low analyte concentrations. Furthermore, electrode arrays can be used to measure multiple analytes simultaneously. Carbon paste electrodes (CPEs) have been successfully applied in a broad range of biological applications because they resist biofouling and a have a large working potential range.[8,9]

Here we have integrated CPEs into a multilayer microfluidic device in order to provide temporally and spatially resolved analysis of a single analyte as an initial step toward making measurements of biologically generated spatiotemporal chemical gradients. The multilayer device (Fig. 1) is capable of both generating and sampling chemical gradients. All three layers are fabricated from poly(dimethyl)siloxane (PDMS) using standard soft lithography processes.[10] Two syringe pumps are used to deliver liquid to a 2-channel input, 8-channel output gradient generator. The 8 output channels of the gradient generator are introduced into a larger main chamber connected to the primary device outlet. A series of 4 vertical sample ports equally spaced in a line orthogonal to the fluid flow direction lead to 4 individual microchannels each oriented orthogonal to a 3-electrode CPE array. Electrodes were fabricated using graphite, carbon nanotubes, and a binding agent using previously published methods.[11] A detailed description of the channel geometries and dimensions can be found in the ESI.†

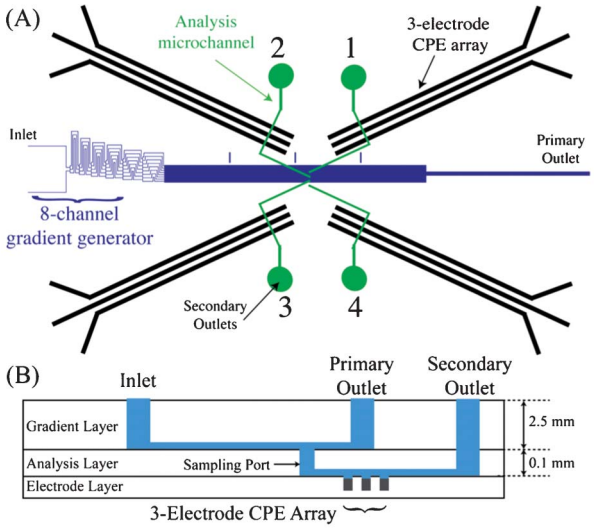

Fig. 1 Diagram of the device used in this study. (A) Top and (B) side view of the 3 separate layers used within the device. All three layers are irreversibly bonded to one another. A 130 μm diameter punch is used to create the vertical sampling ports.

The viscous resistance of the system was designed such that, for pressure driven flow, 50% of the fluid will flow through the main chamber and exit through the primary outlet, and 12.5% of the fluid will flow through each analysis microchannel into a secondary outlet. With this design, the flow through the sample ports will have no effect on the shape of the upstream chemical gradient (see ESI† for details). The design of this system allows for continuous sampling from the 2 mm wide main chamber to monitor real-time changes in analyte concentrations from 4 distinct lateral locations. We have utilized the software package COMSOL to model the transport of both fluorescein and dopamine in this device (ESI†). For the flow rates used in this study, each sample port will collect all analytes situated near the floor of the channel within a distance slightly larger than the diameter of each sample port. This area of analyte collection can be easily modified by adjusting the viscous resistance of the analysis microchannels (*e.g.* by extending the length of each analysis channel). The multilayer approach taken in this study is preferred over placing electrodes directly into the main chamber because it isolates the bulk of each electrode from the chamber and allows for multiple analytes to be quantified from the same spot using expandable electrode arrays.

We utilized time-dependent injections of dopamine to test the ability of the underlying CPE arrays to provide temporal and spatial characterization of chemical gradients present in the main chamber. Two syringe pumps were used to pump phosphate buffered saline (PBS, 1X) solution in equal proportions into each inlet (10 μL min^{-1} per pump). A two-way, six-port valve with a 10 μL injection loop was then used to introduce dopamine solutions of varying concentrations into one side of the gradient generator. The gradient generator has been designed such that upon injection dopamine will be transported through each microchannel (in each successive branch of channels) at similar rates. Therefore, the concentrations of dopamine passing over each sample port will be proportional to one another, and furthermore, that proportionality will not be a function of time.

After injection, dopamine was detected amperometrically on each CPE electrode array *via* the oxidation of dopamine to dopamine-*o*-quinone (0.6 V applied potential *vs.* carbon paste pseudo reference electrode), resulting in a time-series current recording for each sample port. The peak current for all sampling ports with respect to the amperometric detection of decreasing concentrations of dopamine in 1X PBS is shown in Fig. 2. As expected, the peak current decreases with decreasing dopamine concentration. Furthermore, the peak current also decreases with decreasing sample port number, where the proportionality of the responses across all sample ports is not a function of injection concentration. Plots of time-series injections for the 5 different concentrations seen in Fig. 2 can be found in the ESI.† The inset in Fig. 2 displays the time-series response to all four CPE arrays for a dopamine injection of 250 μM. The overall length from the injector to the sample ports is approximately 125 mm (compared to only 7.3 mm from each sample port to CPE array), and it may be assumed that the axial dispersion seen in the inset of Fig. 2 is primarily a result of the longer channels upstream of the ports.[12] Therefore we can infer a relationship between the peak current on each electrode and the concentration of dopamine passing over each sample port.

Fig. 2 demonstrates the ability of this device to sample a chemical gradient in 4 separate locations. Unfortunately, due to the effects of diffusion, the shape of the dopamine gradient near the sampling ports cannot be predicted analytically. To determine the overall shape of a chemical gradient created in this device, fluorescein was added to one of the inputs (0.1 mg mL^{-1}) and the system analyzed using fluorescent microscopy. Because fluorescein (5×10^{-6} cm^2 s^{-1}) and dopamine (2.7×10^{-6} cm^2 s^{-1}) have similar diffusivities, the experimental shape of the fluorescein gradient will be similar to a dopamine gradient tested under the

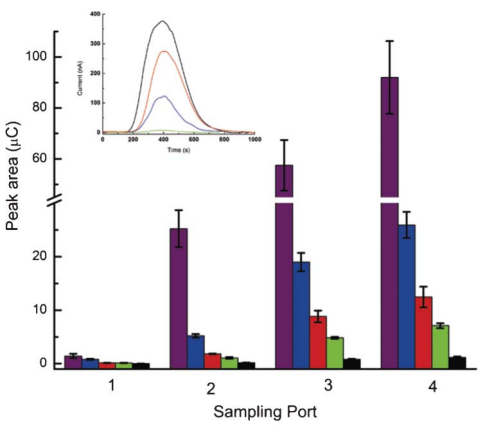

Fig. 2 Peak area *vs.* sampling port for dopamine concentrations (10 μL injections) of 1 mM (■), 250 μM (■), 100 μM (■), 50 μM (■), and 10 μM (■). The error bars represent the standard deviation of 3 separate injections at each concentration. Inset: Current *vs.* time for a single 250 μM injection of dopamine for all 4 sample ports.

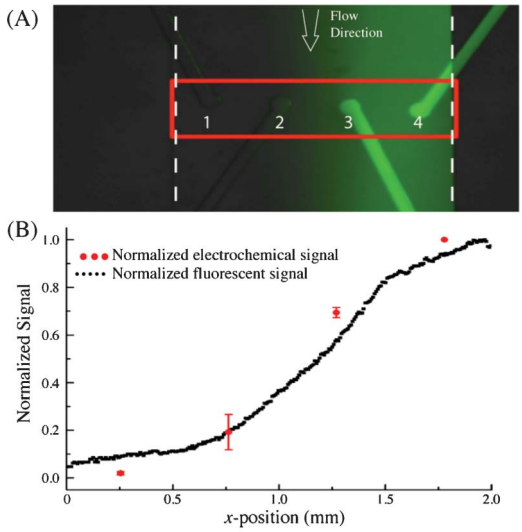

Fig. 3 (A) Fluorescent micrograph of gradient at sampling ports (2.3 cm from gradient network outlet). Dashed white lines indicate fluidic channel walls. Red box indicates the location of the four 130 μm diameter vertical sampling ports. Numbered from left to right, ports 1–4 are at 0.25, 0.76, 1.27, and 1.78 mm from the left channel wall, respectively. (B) Comparison of the normalized fluorescent intensity *vs.* *x*-position taken from image in A (black points) to the normalized signal obtained from the detection of dopamine by the CPE array (red points).

same conditions (buffer composition, flow rate). This similarity has been confirmed with COMSOL, where the concentration profile across the width of the channel is detailed in Fig. S2 and S3, ESI.† Fig. 3A displays a fluorescent image of a steady-state fluorescein gradient in the vicinity of the four sample ports, and it can be seen that the fluorescein concentration decreases monotonically across the width of the channel. These data agree well with the COMSOL predictions, both for the fluorescein and dopamine results.

To allow for direct comparison with the fluorescent line scan data, the signal at each set of electrodes was normalized to the signal at port 4, which was the highest magnitude for each of the five concentrations. The four port values for each concentration were then averaged and reported here as the mean ± SD. Likewise, the fluorescent data was normalized to the maximum intensity across the channel and plotted as a function of *x*-position (distance across the main chamber). As seen in Fig. 3B, there is good agreement between the fluorescent line scan and the amperometry data collected from the device. It should be noted that the amperometric data represents replicate injections at five different concentrations of dopamine.

The slight deviations between the fluorescent and amperometric data shown in Fig. 3B can perhaps be attributed to the 1.9× difference in diffusivity between fluorescein and dopamine. The lower diffusivity of dopamine results in less band broadening of the overall gradient (across the width of the channel), resulting in lower and higher concentrations at the left and right side of the channel, respectively, when compared to a fluorescein gradient.

The dopamine detection limit in this system was determined by injecting homogeneous concentrations of dopamine through both of the gradient introduction ports. The chemical gradient in the main flow channel is eliminated and a uniform concentration of dopamine at each sampling port is established. Using this method, the lowest detectable dopamine concentration (S/N = 3) was found to be 250 nM. This detection limit is high relative to other hybrid microfluidic electrochemical systems due to several factors.[11] First, the laminar flow through the gradient generator will contribute to a measurable level of axial dispersion. Second, the electrode channels were not completely filled with carbon paste, resulting in the potential for analyte flow over the broader electrode and increased baseline noise. In the future, this limitation will be addressed *via* improved fabrication methods. By doing this, we anticipate being able to achieve detection limits closer to that seen previously (~10 nM) with similar CPEs.[13] Regardless of the current detection limits, spatiotemporal gradients in dopamine were measured effectively and these provide a solid foundation for future measurements of biologically generated gradients.

Conclusions

The microfluidic carbon-microelectrode system described here demonstrates the ability of this sampling method to measure the spatial and temporal distribution of both fluorescent and electrochemically active molecules within a fluidic gradient system. While only four sampling ports were used in this proof of concept device, the position of each sampling port can be accurately modified to sample liquid from specific regions of interest. We are presently incorporating cell cultures into this system and using a gradient to deliver compounds with known biological activity to monitor changes in extracellular metabolites. This new system will help quantify dose-response relationships between drugs and tissue/cell cultures more rapidly than traditional microplate methods. Furthermore, it will allow us to gain insight into the intricate biological signaling mechanisms involved in cellular response to external chemical stimuli and allow us to spatially resolve small molecule release and movement during tissue development. It should also be noted that due to the design of the underlying microfluidic layer, this type of device could be used with most detection methods using a planar design, including optical, mechanical, or other electrochemical methods.

References

1 R. L. Caldwell and R. M. Caprioli, *Mol. Cell. Proteomics*, 2005, **4**, 394–401.
2 J. Pihl, M. Karlsson and D. T. Chiu, *Drug Discovery Today*, 2005, **10**, 1377–1383.
3 H. Mao, P. S. Cremer and M. D. Manson, *Proc. Natl. Acad. Sci. U. S. A.*, 2003, **100**, 5449–5454.
4 N. Li Jeon, H. Baskaran, S. K. W. Dertinger, G. M. Whitesides, L. Van De Water and M. Toner, *Nat. Biotechnol.*, 2002, **20**, 826–830.
5 I. Barkefors, S. B. Le Jan, L. Jakobsson, E. Hejll, G. Carlson, H. Johansson, J. Jarvius, J. W. Park, N. Li Jeon and J. Kreuger, *J. Biol. Chem.*, 2008, **283**, 13905–13912.

6 J. Pihl, J. Sinclair, E. Sahlin, M. Karlsson, F. Petterson, J. Olofsson and O. Orwar, *Anal. Chem.*, 2005, **77**, 3897–3903.
7 S. Takayama, E. Ostuni, P. LeDuc, K. Naruse, D. E. Ingber and G. M. Whitesides, *Nature*, 2001, **411**, 1016–1016.
8 A. Morrin, A. J. Killard and M. R. Smyth, *Anal. Lett.*, 2003, **36**, 2021–2039.
9 M. Pumera, A. Merkoci and S. Alegret, *Electrophoresis*, 2007, **28**, 1274–1280.
10 Y. Xia and G. M. Whitesides, *Angew. Chem., Int. Ed.*, 1998, **37**, 550–575.
11 J. J. P. Mark, R. Scholz and F.-M. Matysik, *J. Chromatogr., A*, 2012, **1267**, 45–64.
12 G. Taylor, *Proc. R. Soc. London, Ser. A*, 1953, **219**, 186–203.
13 Y. Sameenoi, M. M. Mensack, K. Boonsong, R. Ewing, W. Dungchai, O. Chailapakul, D. M. Cropek and C. S. Henry, *Analyst*, 2011, **136**, 3177–3184.